Development of antimicrobial/antioxidant nanocomposite film based on fish skin gelatin and chickpea protein isolated containing Microencapsulated Nigella sativa essential oil and copper sulfide nanoparticles for extending minced meat shelf life

Iraj Karimi Sani (eng.irajkarimi@gmail.com)
Urmia University
Nabil Hussain Rasul
Salahaddin University- Hawler
Amirafshar Asdagh
Urmia University
Sajad Pirsa
Urmia University
Naser Ghazanfarirad
Urmia University of Medical Sciences

Research Article

Keywords: Fish skin gelatin, Chickpea protein isolated, Nigella sativa essential oil, Copper sulfide nanoparticles, Active packaging, Minced meat

Posted Date: March 25th, 2021

DOI: https://doi.org/10.21203/rs.3.rs-337479/v1

Development of antimicrobial/antioxidant nanocomposite film based on fish skin gelatin and chickpea protein isolated containing Microencapsulated *Nigella sativa* essential oil and copper sulfide nanoparticles for extending minced meat shelf life

Iraj Karimi Sani[1], Nabil Hussain Rasul[2], Amirafshar Asdagh[1], Sajad Pirsa[1]*, Naser Ghazanfarirad[3]

[1]Department of Food Science and Technology, Faculty of Agriculture, Urmia University, P.O. Box 57561-51818, Urmia, Iran.

[2] Department of Food Technology, College of Agricultural Engineering Sciences, Salahaddin University-Erbil, Kurdistan Region, Iraq.

[3] Master of Biochemistry Food and Drug administration, Medical University of Urmia.

* Corresponding author Email: S.pirsa@urmia.ac.ir, pirsa7@gmail.com

Abstract

Fish skin gelatin and chickpea protein isolated (G-CP) edible blend films incorporated with 0.25 and 0.5% copper sulfide nanoparticle (CuSNP) and *Nigella sativa* essential oil (MEO) (0.015 and 0.03%, w/w of protein) were prepared and optimized by the response surface methodology based on the central composite design (RSM-CCD). Antimicrobial activity, infrared spectroscopy (FTIR), X-ray diffraction (XRD), morphological characteristics and thermal attributes of composite films were examined. In general, the effect of CuSNPs and MEO on the properties of blended films, besides their inherent nature, is related to their interactions with the protein matrix and the synergistic effect on each other. As authenticated by the FTIR and XRD, the simultaneous use of CuSNPs and MEO because of the synergistic effect of CuSNPs on the antibacterial attributes of MEO and raising the content of antimicrobial components in the blend film expressed the highest antimicrobial functionality against *E. coli*. and *S. aureus*. Also, the results of microbiological and chemical tests of packaged minced meat revealed that the simultaneous use of MEO and CuSNP in the film has a positive synergistic effect in increasing the storage life of minced meat, as compared to the other samples.

Keywords: Fish skin gelatin; Chickpea protein isolated; *Nigella sativa* essential oil; Copper sulfide nanoparticles; Active packaging; Minced meat

1. Introduction

To prolonging the shelf life and storage life of food products and decreasing the hazard of food-borne ailments, wrapping plays an essential role in preventing and limiting physical damage and microbial pollution [1]. Petroleum-based plastics because of their good mechanical attributes and the satisfying barrier properties against gases and water are the most widely used food packaging material. However, the accumulation of non-biodegradable plastics leading to serious environmental issues [2]. In the past few decades, developing edible film using natural compounds including flavonoids, polyphenols, proteins, fats and polysaccharides or the simultaneous use of these ingredients has been considered as a promising alternative to petroleum-based plastics [2-3].

Among these biopolymers, proteins, because of their abundance, suitable barrier characteristics against gases and volatile compound and good film-forming ability, and diversity of amino acid composition which can lead to a wide range of interactions and chemical modification reactions, have been extensively utilized for the improvement of properties of edible wrapping films [4]. The high price of animal protein has pushed the researchers to be in search of cheap sources of protein for the fabrication of edible film packaging. Considering this issue, the isolated plant proteins such as chickpea protein and the gelatin isolated from maritime protein sources by-products such as fish skin are promising alternatives [5]. Gelatin is a class of protein fractions that can be derived from the degradation of collagen. Fish skin gelatin had a poor gelling attribute, in comparison to the bovine bone, bovine hide, and porcine skin. However, it has reached more consideration as a material for the production of biodegradable films. So, its usage as film-forming material can also extend its applicability [6]. Recently, chickpea seed has been considered as a remarkable plant protein source, due to its higher protein content (18-25%)

Compared to other grains, relatively low levels of antinutritional factors, high protein bioavailability, the suitable balance of amino acids, and low price [5]. Chickpea protein isolate application as a film-forming component was barely investigated. Nevertheless, as reported by Meshkani, Mortazavi, and Pourfallah [7] it can form edible films with an attractive appearance and good mechanical attributes. However, protein-based films due to their hydrophilic nature normally have poor water resistance properties, which is limiting their usage as potential packaging material. To improve these drawbacks and induce additional advantages such as antibacterial and antioxidant properties to protein-based edible packaging films, the incorporation of lipophilic and hydrophobic materials such as essential oils and metal nanoparticles have been investigated widely [8].

Nigella sativa, which is also known as black seed, is an annual flowering herbaceous plant belonging to the Ranunculaceae family. Its seeds have a high content of phenolic ingredients and are a wealthy source of essential fatty acids and fat-soluble bioactive [9]. Monoterpenes, including α-thujene, pcymene, γ-terpinene, α-pinene, carvacrol and thymoquinone are the main components of the black seed essential oil composition. Thymoquinone is the most abundant compound of the essential oil which is the principal responsible for the essential oil's antioxidant effects [10].

Also, to date, to induce antibacterial attributes to biodegradable edible films, the incorporation of various metallic compound nanoparticles, has been implemented [11-12]. Among them, copper nanoparticles (CuNP) because of their excellent antimicrobial activity, ease of manufacture, and low-cost have shown promise in this field [13]. However, recent investigations have indicated that CuNP is highly toxic to human cell lines. CuSNP nanoparticles are one of the most efficient modified Cu nanoparticles which, their toxicity has been controlled, using

sulfidation of CuNP (CuSNP) [14]. It is a p-type semiconductor with unique optical and photothermal and electrical conversion characteristics. The photothermal effect is attributed to the absorption of light and its release as thermal energy, which can destroy the microorganism cell membrane and denatured the proteins [1].

Minced meat is a highly sensitive food that has a short storage life of a few days in the refrigerator, mainly restricted by microbial growth and lipid oxidation. The high amount of nutrients, moisture, lipid, and protein caused it to be a perishable food raw material [15]. The growth of bacteria can lead to off-odors, off-flavors and slime production. Also, odor, color and flavor alterations from lipid oxidation can limit the shelf life of a food product [16]. Therefore, it seems that the development of an effective antibacterial and antioxidant edible nanocomposite packaging film could be a good strategy to delay the microbial spoilage and fatty acids oxidation in minced meat. Concerning what stated above, the main object of this work is the fabrication of an edible nanocomposite film with antibacterial and antioxidant properties based on fish skin and chickpea protein (G-CP) as cheap sources of filmogenic material, *Nigella sativa* essential oil (MEO), and CuSNP nanoparticles to enhance the shelf life of minced meat.

2. Materials and methods

2.1. Materials

Chickpea seeds (*C. arietinum*) and *Nigella sativa L.* seed essential oil were acquired by Plant Improvement Institute. (Urmia, Iran). Sodium hydroxide (NaOH), hydrochloric acid (HCl), n-hexane (C_6H_{14}), potassium bromide (KBr), reagent-grade absolute ethanol, 2,2-diphenyl-1-picrylhydrazyl 95% free radical, 2-thiobarbituric acid, glycerol, and sodium caseinate purchased from Sigma Chemical Co. (St. Louis, MO, USA). *Escherichia coli* and *Staphylococcus aureus* (O157:H7) was purchased from the Iranian Research Organization for Science and Technology

(Persian Type Culture Collection, Tehran, Iran) and CuSNP nanoparticle (Us Nano Co, USA). All other chemicals materials were of analytical grade.

2.2. *Fish skin preparation*

Fresh bigeye snapper (P. tayenus), fishes were stored in ice and transported within 3 h to the Department of Food Technology of Urmia University. The thawed fishes were washed and cleaned with running tap water just after arrival and fish skins were then scraped and removed. The removed fish skins were cut into small pieces (1×1 cm2), and refrigerated at -20 °C until gelatin extraction.

2.3. *Fish skin gelatin extraction*

Gelatin was extracted from bigeye snapper fish skin according to the technique reported by Rattaya et al. [2] with a minor alteration. The washed skins were immersed in 0.025 M NaOH with a fish skin/solution ratio of 1:10 (w/v) with continuous gentle stirring at ambient temperature. To take off non-collagenous protein and pigments the alkaline solution was switched every 3 h. NaOH-treated skins were then washed by tap water until the neutral wash water (pH of washed water <7.5) was achieved. Then the fish skins were immersed in 0.05 M CH_3COOH with a skin/solution ratio of 1:10 (w/v). The solution was switched every 3 h with a mild stirring to swell the collagenous ingredient of fish skins. CH_3COOH-treated skins were washed as previously described. To extract gelatin, the swollen fish skins were immersed in dialyzed against distilled water (45 °C) with a skin/distilled water ratio of 1:10 (w/v) for overnight with continuous gentle stirring. The combination was then filtered using two layers of cheesecloth and freeze-dried.

2.4. *Chickpea protein isolate (CPI) extraction*

The chickpea protein extraction was prepared according to the methodology described by Mousazadeh et al. [5] with slight modifications. Firstly, for defatting chickpea flour, it was mixed with hexane with continuous stirring two times for 2 h at ambient temperature (1:5 [w/v], chickpea flour: hexane). In the second step, the defatted chickpea powder was suspended in doubly distilled water (1:10 [w/v]) than the pH was adjusted at 10 using 1 N NaOH with subsequent stirring at 1200 rpm for 2 h at room temperature (25 °C). The mixture was centrifuged at 9000 ×g for 30 min and the obtained supernatant was used for the next step. Finally, to precipitate the protein, the pH of the obtained supernatant adjusted at 4 (isoelectric point of CPI) using 1 N HCl and was centrifuged at 8500 ×g for 20 min. The precipitated CPI protein was washed with doubly distilled water two more times and was centrifuged to remove the non-protein components and freeze-dried.

2.5. ***Encapsulation of MEO***

Sodium caseinate was used as the wall materials to encapsulate the MEO. Sodium caseinate was dispersed in deionized water (60 °C) using magnetic agitation and kept overnight at 4 ºC for complete hydration. MEO was gradually added to the solution to prepare a coarse emulsion. Afterward, the mixture was pre-homogenized using a homogenizer (Silverson L4R, Buckinghamshire, England) for 10 min at 5000 rpm. Finally, to provide a fine emulsion, the coarse emulsion was prepared whit a high-pressure homogenizer (AH100D, ATS Engineering Inc., Canada) at 300 and 250 MPa, and spray dried to provide the dried powder of MEO.

2.6. ***Preparation of nanocomposite films***

The composite edible films were made utilizing a casting methodology. First, 2.5 g of gelatin and 2.5 g of CPI powder were added to 100 ml of pure water. The pH of the produced dispersion

was adjusted to 8 with 0.1 N NaOH and, the blend was stirred on a magnetic stirrer for 20 min at 90 °C to ensure its denaturation. Afterward, the encapsulate MEO (0–0.5%) was added to the dispersion and a homogenizer device (Avestin Inc., Ottawa, Canada) was utilized to combine the dispersion for 10 min at 10000 rpm. Then the CuSNPs (0–0.03%w/v) were added to the dispersion and it was combined by a magnetic stirrer for 15 min and then settled in an ultrasonic bath for 15 min to ensure homogeneous distribution of CuSNPs. Finally, glycerol (40% w/w dry matter) was added, and the dispersion was mixed by a stirrer for 30 min. The achieved blend was ventilated for 10 min and 25 ml of it was poured into the center of the petri dish and was dried at room temperature for 2 days. The dried films were equilibrated at ambient temperature and 50% relative humidity (RH) until further analysis.

2.7. ***Thickness***

The films thickness was determined by a digital micrometer (QLR digit-IP54, China) with 0.001 mm of accuracy at ten random locations of each blend film sample. Average values were used for other calculations [17].

2.8. ***DPPH radical-scavenging activity (RSA)***

The antioxidant activity of the blend digestible films was ascertained utilizing the DPPH methodology [18]. In Brief, 50 mg of blend film samples were dissolved in 10 ml of water. After that, 0.2 ml of blend film extracts solutions were united to 7.8 ml of the DPPH solution (0.1 M methanol solution), and then, the solutions were saved in the dark at 25 °C for 1h. Finally, the absorbance was measured against pure methanol at 517 nm. The percentage of DPPH radical-scavenging activity was estimated by the following formula:

$$\text{DPPH scavenging activity (\%)} = \left(\frac{A_{blank} - A_{sample}}{A_{blank}}\right) \times 100 \quad (1)$$

where A_{blank} is the absorbance of the control, and A_{sample} is the absorbance of the test compound.

*2.9. **Moisture content***

The blend films moisture content was estimated by measuring the lose-weight of preconditioned edible films after drying in an oven at 103 ± 2 °C to the point that reaching a constant weight [19]:

$$MC = \frac{M_1 - M_2}{M_1} \times 100 \quad (2)$$

where, M_1 is the preconditioned film sample weight and M_2 is dry film sample weight.

*2.10. **Water vapor permeability (WVP)***

The composite films WVP was evaluated utilizing the standard gravimetrical methodology of E96 (ASTM, 1995) [20], with little modifications according to the equations of Chavoshizadeh [21]. Composite film samples were sealed tightly with parafilm on the top of the cups, which were filled with approximately 35 g of anhydrous $CaCl_2$ to provide relative humidity (RH) of 0%. Thereafter, the glass cups were stored in a saturated NaCl solution desiccator (75% RH) at ambient temperature. The difference in RH of the two sides of the blend films corresponds to a driving force of 1753.55 Pa, expressed as water vapor partial pressure. The weighing was performed every 1h until 8 h and then every 8 h until 48 h. The increase in weight of cups was plotted against time and the Slopes were determined by linear regression. The WVP was calculated in accordance with the following equation and expressed as g m^{-1} s^{-1} Pa^{-1}.

$$WVP = \frac{\Delta m.X}{\Delta t.\Delta p.A} \quad (3)$$

where $\Delta m/\Delta t$ is the weight of moisture gain per unit of time (g/s), X is the average composite film thickness (m), A is the area of the exposed composite film (m^2), and Δp is the partial vapour pressure difference between the two sides of the composite film (Pa).

2.11. ***Color parameters***

A colorimeter (D25-9000, Hunterlab, U.S.) was utilized to assess the color values of composite film samples. Edible film samples were located on a white standard plate (L* = 95.49, a* = -0.30 and b* = -0.08) and values of L* (brightness), a (redness-greenness) and b (yellowness-blueness) of films were determined. The total color difference (ΔE) was measured by the following Eqs: [22].

$$\Delta E = \sqrt{[(L - L^*)^2 + (a - a^*)^2 + (b - b^*)^2]} \quad (4)$$

2.12. ***Mechanical properties***

The preconditioned blend films mechanical behavior including tensile strength (TS) and elongation at break (EAB%) were estimated utilizing Texture Analyzer (Stable Micro System, Surrey, UK) according to ASTM standard technique D882 (ASTM, 2001) [23].TS and EAB were calculated as follows:

$$TS = \frac{F}{A} \quad (5)$$

$$EAB = \frac{\Delta L}{L} \times 100 \quad (6)$$

where, F (N) is the maximum stress that the blend film samples can withstand; A (m^2) is the cross-sectional area of the film samples (thickness × width); ΔL is the increase in length at the breaking point; and L is the initial length between the grips.

2.13. *Evaluation of antimicrobial activity of films*

In order to estimate the antibacterial activity of the blend films was evaluated utilizing an agar disk diffusion technique, according to the methodology reported by Mehmood, Sadiq, and Khan [24]. The composite film samples were cut into 2×2 cm^2 pieces and settled on a special plate of Mueller-Hinton Agar plates (Merck), which was inoculated with 0.1 mL of broth cultures comprising approximately 105 –106 CFU/mL of *E. coli O157: H7* and *S. aureus* bacteria. The agar plates were incubated at 36 ± 2 °C for 1 day. The area of inhibition zones (mm) around the composite film pieces was estimated taking into account the primary diameter of the blend films.

2.14. *Fourier transform infrared spectroscopy (FT-IR) analysis*

To determine the chemical composition, preliminary structures and possible interaction between the components of the composite films, the FTIR spectra of composite films were registered by the FT-IR spectrophotometer (EQUINX55, Brucher, Germany). The FTIR spectra were recorded over at the wavenumber range from 600 to 4000 cm^{-1} with 4 cm^{-1} resolutions [25].

2.15. *X-ray diffraction (XRD) analysis*

To assess the crystalline structures of the blend film samples, there X-ray patterns were measured utilizing an XRD diffractometer (RINT2000, Tokyo, Japan). The composite film samples were scanned at the diffraction range (2θ) of 10° to 80° [26].

2.16. *Morphological characterization (SEM)*

The morphological characteristics (surface and cross-sectional) of the composite film samples were analyzed by a scanning electron microscope (S-4800, Hitachi, Japan) at a magnification of 5000× and acceleration voltages of 10 kV [27].

2.17. ***Differential scanning calorimetry (DSC)***

DSC of blend film samples was done on a thermogravimetric analyzer (Shimadzu Scientific Instruments, 154 Kyoto, Japan) in an Ar atmosphere. In this analysis, the blend film samples were heated (25 to 300 °C) with a heating rate of 10 °C/min.

2.18. ***Preparation of minced meat***

The minced beef meat was provided from a local butchery and moved to refrigerator condition (4 °C) within 1h. Then, the minced meat samples (50 g) were afforded under aseptic positions and wrapped with edible composite films. Following that, the wrapped minced meat samples were located in permeable polyethylene bags and stored in the refrigerator at 4 °C for 10 days. Also, the minced meat sample without composite film was applied as a control sample [16].

2.19. ***Physicochemical analyses of minced meat***

2.19.1. ***pH value***

5 g of the various minced meat samples were mixed with 45 ml of distilled water and the pH of the mixture was measured utilizing an electronic pH-meter (pH-30 sensor; Corning, Lisboa, Portugal) [28].

2.19.2. ***Determination of 2-thiobarbituric acid (TBA)***

2-Thiobarbituric acid (TBA) (mg malonaldehyde/kg (MDA/kg) minced meat) was determined according to the methodology defined by Kirk and Sawyer [29] with minor alteration. Briefly, minced meat (10 g) was homogenized with 20 mL of TBA solution (15% trichloroacetic acid, 0.375% TBA). The compound was boiled for 1 h in boiling water (90 ◦C) and then cooled with running water at ambient temperature and centrifuged at 4200 ×g for 15 min. The absorbance of the final reaction solution was recorded at 532 nm applying a UV-1601 spectrophotometer

(Shimadzu, Kyoto, Japan). TBA values of the minced meat were estimated from the standard curve of malondialdehyde per kg of meat (mg MDA/kg meat). Three replicate was performed for each minced meat sample.

2.19.3. ***Determination of total volatile basic nitrogen (TVB-N)***

The total volatile base nitrogen (TVB-N) content of minced meat samples was measured according to the methodology of AOAC [30]. Ultimately, TVB-N contents were reported as mg nitrogen/ 100 g of minced meat samples. Three replicates were accomplished for each sample.

2.20. ***Bacteriological analysis of minced meat***

At 1, 4, 8, and 14 days of storage, 20 g of each minced meat sample were mixed with 180 ml of 0.1% peptone water in a stomacher-400 (Seward Ltd, Worthing, UK) for 1 min. Ten-fold serial dilution was performed and cultured in Selective media. Then, the plates were incubated under certain conditions. Selective media, incubation temperature and time were as follows: *Enterobacteriaceae* in Violet Red Bile Glucose (VRBG) agar (30 °C for 1 day), *Psychrotrophic* bacteria in plate count agar (6 °C for 10 days), *S. aureus* in Baird Parker agar (38 °C for 2 days). Microbiological enumeration outcomes were reported as logarithms of Colony Forming Units (cfu/g) minced meat [15].

2.21. ***Statistical analysis***

The statistical measure was done in 2 segments. In the first part; The MEO concentration (in 3 levels) and CuSNPs concentration (in 3 levels) were considered as independent parameters to study their effect on the thickness, RSA, WVP, moisture content, and color properties of edible composite films applying a central composite design (CCD) (Table 1). Statistical equations, data analysis (at 95% confidence level) and drawing of diagrams were performed by Design Expert

11.0.0 program. In the second part; a completely randomized factorial design was used to investigate the effect of MEO and CuSNPs on the different properties of composite films (Table 1). The IBM© SPSS® program version 18.0 was employed to perform the examination of variance (ANOVA) tests. The differences comparisons between mean values were established by Duncan's multiple range tests at $p < 0.05$. All experimental data were executed in triplicate and values were reported as mean ± standard deviations.

3. Results and discussion

3.1. ***Thickness, RSA, WVP, moisture content and color properties of composite films***

Table 2 explains the mathematical equations that represent the relationships among MEO and CuSNP on thickness, RSA, WVP, moisture content, and color properties of the gelatin-chickpea protein (G-CP) based film. Fig. 1 and Fig. 2 shows the 3-D response surface plots of the effect of MEO and CuSNP on the thickness, RSA, WVP, moisture content and color properties of G-CP-based film. As shown in Fig. 1, the thickness of G-CP films incorporated with MEO increased significantly with the rising level of MEO, this is maybe due to the increase in the solids content of the films. In contrast, the addition of CuSNP to the composite film reduces the thickness of the blend film, so that the edible film that has the highest level of MEO and the lowest amount of CuSNP has the highest thickness. The findings were in accordance with the result reported by Asdagh et al. [31], which revealed that by raising the ratio of coconut essential oil, the thickness of nanocomposite films based on whey protein/copper oxide nanoparticles increased. Also, Karimi Sani, Pirsaa, and Tağıb [3] reached similar findings, with the increase in the level of *Melissa officinalis* essential oil, the thickness of chitosan composite films increased.

Lipid oxidation is a major problem in fatty foods such as meat, fish, and dairy products, so the application of films containing antioxidants compounds like MEO and CuSNP can be very

311 effective in solving this problem. Antioxidative activity of G-CP based films in the different
312 levels of MEO and CuSNP is presented in Fig. 1. In the present study, the DPPH was used to
313 evaluate the antioxidant activities of the bioactive films. In general, essential oils have high
314 phenolic compounds, which means their high antioxidant power. Kadam, Shah, Palamthodi, and
315 Lele and Akloul, Benkaci-Ali, Zerrouki, and Eppe [32-33] studied the antioxidative effect of
316 *Nigella sativa* essential oil. The incorporation of MEO significantly raised the DPPH radical
317 scavenging activity of G-CP films. The antioxidant effect of MEO might be due to the presence
318 of an aromatic nucleus containing polar functional groups in its components (including
319 thymoquinone, carvacrol, trans-anethole, and 4-terpineol) (Singh, Marimuthu, de Heluani, &
320 Catalan, 2005). On the other hand, the DPPH radical scavenging activities of G-CP films
321 containing CuSNP were higher stronger than G-CP films containing MEO, this shows that
322 CuSNP could enhance the antioxidant activity of films by accepting or donating electrons. From
323 the results obtained on the antioxidant properties of film samples containing MEO and CuSNP,
324 it can be concluded that produced active films are a suitable option for protecting the wrapped
325 food against free radical-induced oxidation.

326 WVP is one of the most important parameters in the determination of the amount of water
327 transmission of the edible films. An important performance of biopolymeric films is to decrease
328 the exchange of moisture between the wrapped food and outside packaging environment, hence
329 the water loss of product can be decreased [34]. The results of the WVP values of the films are
330 shown in Fig. 1. The effect of MEO and CuSNP on the WVP of the G-CP films shows a
331 contradicting effect at the different levels studied. The results indicate a rise in the values of WVP
332 of G-CP-MEO blended films compared to G-CP-CuSNP films. The WVP of the films increased
333 with a raise in MEO levels, which probably due to the interactions of -OH and COO^- groups of

NSE with the active sites (amino groups) in G-CP. These interactions, in turn, may have led to diminished interactions between G and CP in the film matrix, thus reducing film integrity and, consequently, reducing the WVP values. A similar phenomenon was observed in chitosan-based films containing *Nigella sativa* [32]. Initially, the WVP decreases with increasing CuSNP levels but increased with further increases content of CuSNP. The reduced WVP values of the active blended films at low levels of CuSNP was maybe because of the tortuous path of moisture diffusion created by the well-distributed moisture vapor impermeable CuSNP [14]. Nevertheless, the increased WVP values of the bioactive films at the high percentage of CuSNP was mainly due to the agglomeration of the CuSNP, and interaction between CuSNPs has decreased the number of SH-bonds between active groups of protein matrix (G-CP) [35].

Low moisture content composite films facilitated and accelerated the wrapping of water sensitive food materials [36]. The moisture content of G-CP based films is presented in Fig. 1. Our results indicated that with raising MEO levels, the moisture content of composite films reduced. This may be because of the interactions of -OH and COO^- groups of MEO with the -OH and $-NH_2$ in the G-CP polymeric matrix. This interaction, in turn, may have led to decreased interactions between G-CP and moisture molecules. These results were similar to those achieved by Kadam et al. [32] for chitosan-based films. Similarly, reduction in moisture contents of the CuSNP-containing films with increasing CuSNP levels could be explained by the arrangement effect made between the copper atom and -OH/$-NH_2$ groups in the G-CP matrix, which also limited the interactions between hydrophilic groups in G-CP and water molecules. A similar result was observed in the chitosan film incorporated with silver nanoparticles and purple corn extract [37].

356 The colorimetric results in Fig. 2 show that the color parameters of the G-CP films are
357 strongly affected by incorporation CuSNP, but the addition of MEO does not effect on the color
358 of the produced G-CP-based films. The brightness parameter L* reduces with a raising of the
359 level of CuSNP. Also, as CuSNP content increased, a* and b* parameters were enhanced.
360 Additionally, the total color difference (ΔE) of the G-CP films was enhanced with an increased
361 percentage of CuSNP. This observation is in agreement with those reported by Roy et al. [14] for
362 the agar-based-CuSNP-containing film.

363 *3.2.* ***Mechanical properties***

364 An edible film with desirable properties must have high tensile strength (TS) and elongation
365 at break (EAB). The type of polymeric matrix and type and degree of interactions between
366 ingredients influence on the mechanical behavior of blend film [22]. The TS and %EAB of G-
367 CP-based blend films are shown in Table 3. The addition of MEO decreased the TS and increased
368 %EAB. This indicated molecular interactions (electrostatic interactions and ester linkages)
369 between MEO and G-CP chains, these, in turn, affect the protein-protein chain interactions and
370 provide the flexible domains within the composite films with the lesser tensile strength [32]. After
371 incorporation of CuSNP in G-CP composite film, TS and EAB% decreased (Table 3). This can
372 be attributed to the aggregation of the nanoparticles, as observed in the SEM results (Fig. 3. C)
373 [38]. Due to the synergistic effect of MEO and CuSNP, G-CP-MEO 0.5-CuSNP 0.03 film
374 exhibited the highest TS than other active films (G-CP-MEO 0.5 and G-CP-CuSNP 0.03) ($p <$
375 0.05).

376 *3.3.* ***Antimicrobial property***

377 The antimicrobial attributes of the G-CP-based blend films were examined versus both Gram-
378 positive (*S. aureus*) and Gram-negative (*E. coli*) microorganisms, and findings are shown in

379 Table 3. Results of the inhibition zone revealed that, in general, blending G-CP edible film with
380 the MEO and CuSNP caused effective antibacterial activity versus the *S. aureus* and *E. coli*. As
381 anticipated, the G-CP composite film did not show any antibacterial activity, but G-CP films
382 containing MEO and CuSNP showed varied antibacterial activity depending on the variety of
383 bacteria. The GCP-CuSNP 0.03 composite films demonstrated stronger antibacterial activity
384 against *E. coli* than *S. aureus*. A comparable effect of antimicrobial activity was observed in
385 alginate-based composite films blended with CuSNP [38]. The various antibacterial action of
386 CuSNP depending on the type of bacteria is maybe because of the different cell wall structures
387 and morphological differences of these bacteria [13]. The Gram-negative organisms are
388 composed of complex cell wall structure with a thin peptidoglycan layer surrounded by an outer
389 phospholipidic membrane, on the contrary, the Gram-positive organisms have a thick cell wall
390 structure with a multilayer of peptidoglycan [14]. Although until now antibacterial activity of
391 CuSNP has not been clearly outlined yet and not clearly understood, however, it is believed that
392 free copper ions (Cu++) be able to interact with the negatively charged microorganism cells
393 membrane protein and demolish the microorganism cell wall [38]. Another possible mechanism
394 is the antioxidant defense or interaction antioxidant defense of CuSNP with bacterial, which
395 activates intracellular reactive oxygen species-mediated oxidative damage to antioxidant
396 resistance and damages bacterial cell membranes, leading to microbial cell death [14]. The results
397 of the antibacterial activity of films containing MEO show that *S. aureus* is more sensitive against
398 MEO than *E. coli*. As mentioned earlier, the reason for this difference could be allocated to the
399 morphological distinction among the bacteria, as a result, Gram-negative organisms like *E. coli*
400 due to having an outer layer of phospholipid membrane that carrying the lipopolysaccharide
401 ingredients makes the cell wall strong and impenetrable to lipophilic compounds like MEO [39-

40]. The antimicrobial mechanism of the essential oils (MEO) is also attributed to the disabling of the cytoplasmic membrane and disrupting of the cellular energy metabolisms [39] Notably, G-CP/MEO/CuSNP film exhibited the strongest antibacterial property ($p < 0.05$), indicating that the synergistic effect of MEO and CuSNP has improved the antimicrobial properties of the film and this active film could be utilized as antibacterial wrapping material in the food industry.

3.4. ***FTIR***

FTIR analysis was used to evaluate the chemical structure and possible interactions between nanocomposite films different components. FTIR spectra of all components individually and FTIR spectra of different produced nanocomposite films were shown in Fig 3. A. As can be seen in Fig 3. A. (a and b) the absorption band at 1245 cm^{-1}, 1546 cm^{-1}, and 1661 cm^{-1} was attributed to the presence of amide-III (C-N and N-H stretching), amide-II (N-H bending), and Amide-I (C=O stretching) functional groups in gelatin and chickpea protein structure, respectively. Also, the wide absorption band at 3600-3100 cm^{-1} was attributed to O-H and N-H vibration stretching [34-5]. The spectrum of incapsulated MEO was shown in Fig 3. A. (c). The sharp asymmetric band occurs at 3100-2850 cm^{-1}, confirmed the presence of aliphatic and unsaturated hydrocarbons in the essential oil structure. The peaks at 1743 cm^{-1}, 1161 cm^{-1}, 1034 cm^{-1} and 851 cm^{-1} can be related to (-C=O) stretch, (-C-O) stretch; ($-CH_2$) bending, (-C-O) stretch and ($=CH_2$) wagging, respectively [41]. The main distinctive peaks which were mentioned above for the control film and MEO spectrum can be observed in the spectrum of the nanocomposite film incorporated with MEO (Fig.3. A. (f and h)). However, some peaks were shifted to a higher or lower frequency or their amplitude changed which is attributed to the conformational changes of functional groups as a result of components' different interactions [34]. As can be seen in Fig. 3.A (g) there are no notable changes in active groups by incorporation of CuSNP. These findings demonstrated that

no new chemical interaction takes place among the other ingredients and CuSNP and the changes in peak intensities could be because of van der Walls or H-bonding among CuSNP and blend film matrix [14].

*3.5. **XRD***

The XRD patterns of the control film (G-CP) showed a broad peak at 2θ of 24°, typical of protein materials which illustrate its amorphous structure (Fig. 3.B-a) [42]. As can be seen in Fig. 3.B-b. by incorporation of MEO the intensity of the mentioned peak slightly decreased which indicates the homogenous distribution of MEO in the nanocomposite film matrix. The XRD pattern of CuSNP showed in Fig. 3.B-c [32]. The peaks at 2θ = 28.1°, 30.4°, 32.4°, 33.5°, 47.9, 54.1°, 60.8° perfectly match up with the (101), (103), (104), (007), (109), (110), and (114) planes of hexagonal phrase of CuSNPs with lattice constants of a =3.780 Å and c =15.37 Å [1]. The mentioned peaks were also can be seen in the XRD pattern of nanocomposite film containing both MEO and CuSNPs (Fig. 3.B-d) which confirm that no new chemical interaction carried out between the other components and CuSNPs [14]. On the other hand, the broad peak at the XRD pattern of control film (G-CP) approximately disappeared in the XRD pattern of this sample which indicated the perfect homogeneous distribution of CuSNP in the proteinous matrix of nanocomposite film.

*3.6. **SEM***

The SEM surface micrographs of prepared nanocomposite films were shown in Fig. 3. C-a. A smooth and homogenous surface without any observable crack was observed for the control film (G-CP). The observed homogenous surface structure indicates that fish skin gelatin and chickpea protein have great compatibility to be mixed. As can be seen in Fig. 3.C-b the surface morphology

447 of nanocomposite film became slightly rough by the incorporation of MEO. The homogeneity of
448 mentioned roughness confirms the homogeneous distribution of MEO droplets in the film matrix.
449 A similar observation was reported by Kadam et al. [32]. As can be seen in Fig. 3.C-c some
450 granular protrusions were appeared by the incorporation of CuSNP, which decreased the
451 uniformity of the nanocomposite film surface. The appearance of granular protrusions was most
452 likely because of the aggregation of some CuSNP [1-14]. The mentioned effects of incorporation
453 of MEO and CuSNP (Fig. 3.C-d) were also observable in the surface micrograph of
454 nanocomposite film containing both MEO and CuSNP.

455 *3.7.* ***DSC***

456 DSC thermal analysis test results of the G-CP- based nanocomposite films are shown in
457 Table 4. The results showed that the addition of MEO and CuSNP in G-CP film significantly
458 increases the melting temperature (Tm) and glass transition temperature (Tg) of the produced
459 films. Also, the simultaneous use of MEO and CuSNP has a significant synergistic effect in
460 improving the Tm of composite films. This increase in Tm and Tg was probably due to the
461 inherent nature of MEO and CuSNP, changes in the degree of crystallinity with incorporation of
462 MEO and CuSNP in protean matrix and increased CuSNP/MEO interactions with G-CP matrix
463 [38-32]. G-CP displayed a Tm of 88 ℃ whereas the all composites showed higher Tm.

464 *3.5.* ***Physicochemical analyses of minced meat***

465 Changes in pH values of fresh minced meat wrapped with G-CP protein-based films during
466 refrigerated storage for 14 days are presented in Table 5. The initial (1 day) pH value of the
467 control film (G-CP) increased from 5.85 to 6.35 after storage for 14 days. Generally, pH of all
468 samples slightly raised, when the storage time increased ($P < 0.05$). Such a raise in pH indicates

469 a degree of minced meat spoilage through higher bacterial growth and microbial enzymatic
470 actions leading to the formation and accumulation of alkaline compounds such as ammonia and
471 amines, etc. [43]. Samples packaged in G-CP films containing MEO and CuSNP alone and in
472 combination with together has lower pH compared to control film (G-CP) throughout the storage
473 period ($P < 0.05$), showing the protective effects of the MEO and CuSNP against substrate
474 decomposition. Also, the pH value in the packaged sample with G-CP composite film enriched
475 with MEO and CuSNP were less than other minced meat samples wrapped with G-CP-MEO 0.5
476 and G-CP-CuSNP 0.03 active films ($p < 0.05$), that this indicates the positive synergistic effect
477 of MEO and CuSNP in the packaging film to reduce meat spoilage. These findings confirm the
478 results of other physicochemical and bacterial analyses of wrapped minced meat and are by other
479 studies [15-43].

480 The effect of G-CP film containing MEO and CuSNP on the changes of TVB-N of minced
481 meat during the 14 days' storage at refrigerated temperature are shown in Table 5. The primary
482 TVB-N of 7.00 mg N/100g values were incremented progressively in all samples ($P < 0.05$), and
483 reached to 37 mg N/100g for G-CP (control sample). Previous studies have reported that the
484 increase of TVB-N with storage period is likely because of spoilage bacteria and the formation
485 of compounds such as dimethylamine, methylamine, ammonia and trimethylamine [44]. As it
486 was observed, TVB-N values in both samples of meat packed in MEO-containing films (G-CP-
487 MEO 0.5 and G-CP-MEO 0.5-CuSNP 0.03) were less than the other samples, although this value
488 in the sample wrapped in G-CP-CuSNP 0.03 film was significantly lower than in the control
489 sample ($P < 0.05$), indicating antibacterial properties of CuSNP. Generally, the lower and
490 acceptable TVB-N values in treated minced meat samples could be associated with the
491 antibacterial activities of examined preservative agents. MEO and CuSNP remarkably reduced

492 the bacterial population of the meat sample than G-CP and subsequently decreased the oxidative
493 deamination and accumulation of non-protein nitrogen and other volatile compounds [45].

494 The changes of TBA values during storage at refrigerated temperature of minced meat
495 wrapped with G-CP or G-CP-MEO 0.5, G-CP-CuSNP 0.03 and G-CP-MEO 0.5-CuSNP 0.03
496 films are presented in Table 5 to evaluate the impact of these films on minced meat lipid
497 oxidation. TBA value has been extensively used to assess the extent of fat oxidation in meat,
498 meat products and meat by-product [46]. The primary TBA value of all treatments was 0.4 mg
499 MDA/kg sample. Generally, TBA values of all minced meat treatments raised regularly up to 14
500 days of storage ($p < 0.05$). However, the minced meat samples wrapped with G-CP-MEO 0.5, G-
501 CP-CuSNP 0.03 and G-CP-MEO 0.5-CuSNP 0.03 films had much lower TBA values, tan sample
502 wrapped with control G-CP film. These findings may be related to the high capacity of the MEO
503 and CuSNP on preventing the oxidation of fatty acids of meat through antioxidant properties and
504 inhibition of microbial growth. Since fat oxidation can be initiated, extended, inhibited or reduced
505 through control of several mechanisms including the enzymatic and non-enzymatic generation of
506 free radicals, production of singlet oxygen and active oxygen [47], the strategy of using MEO
507 and CuSNP in packaging film has been very effective. Also, during the storage time, the TBA
508 values were lower in G-CP active film containing both MEO and CuSNP than in the other ones,
509 this effect confirms the positive synergy of these two compounds for preventing the increase of
510 TBA value due to various reactions, in G-CP based film.

511 *3.6.* ***Bacteriological analysis of minced meat***

512 One of the most important parameters limiting the shelf life of meat is microbial growth [43].
513 As meat bacterial spoilage is initially considered typically a superficial phenomenon, minced
514 meat becomes more sensitive to microbial spoilage via an enlargement in the surface and also the

ease of bacterial entrance from the surface following spreading. Table 5 shows the changes of *L. monocytogenes*, *S. aureus*, *Enterobacteriaceae* and *Pseudomonas spp.* the population of minced meat packaged by G-CP film incorporated with MEO and CuSNP during refrigerated storage. Generally, all films in this study represented significant inhibitory effects ($p < 0.05$) against studied bacteria than the control sample (G-CP). It should be noted that, in all treatments, the bacterial population (*S. aureus*, *Enterobacteriaceae* and *Pseudomonas spp.* population) were considerably increased, except *L. monocytogenes* population, which is decreasing for meat sample wrapped with active films (G-CP-MEO 0.5, G-CP-CuSNP 0.03 and G-CP-MEO 0.5-CuSNP 0.03) over 14 days of storage at different rates ($p < 0.05$). The highest and lowest bacterial population were found for untreated (G-CP film) and treated samples with G-CP containing both MEO 0.5 and CuSNP 0.03 (G-CP-MEO 0.5-CuSNP 0.03) respectively. The following sequence inhibition effect on all studied bacterial groups was found in selected films: G-CP-MEO 0.5-CuSNP 0.03 > G-CP-MEO 0.5 > G-CP-CuSNP 0.03 > G-CP. These findings suggest that MEO and CuSNP could inhibit bacterial growth. Also, the simultaneous existence of MEO and CuSNP in the matrix of the blended film more suppressed the growth of all tested bacterial groups in comparison with the other active films ($P \leq 0.05$). This, as mentioned earlier, shows the antimicrobial synergistic effect of MEO and CuSNP. The antimicrobial effect of MEO is possibly to be related to the effect of a bacterial membrane and leads to changes in the permeability of cations and eventually cell death [39]. Generally, EOs coagulate the cytoplasm, denaturation of cellular proteins and enzymes, and inhibition of DNA, RNA and protein synthesis of bacterial cells and also, disrupt the electron motive force and proton [15]. Also, the adding of CuSNP into the G-CP-based films prevents microbial growth through inhibition of cytoplasmic membrane It should be noted that the function and effectiveness of incorporated MEO and CuSNP in the G-

CP based films through indirect and direct displacement from the film to minced meat depends on the nature of the antibacterial ingredients. Nonvolatile ingredients like CuSNP transfer through diffusion and need direct touch among the films and the minced meat. In contrast, volatile ingredients like MEO release to the headspace, tan penetrate the minced meat surface and are adsorbed into its [15]. Therefore, it can be concluded that this is one of reasons for the greater antimicrobial action and effectiveness of MEO compared to CuSNP. These results are in agreement with those reported by Gomez-Estaca et al. and Ahmad et al. [48-49]. Who observed an antibacterial effect of essential oils to extending the shelf life of the fish and lemongrass essential oil to extend the shelf-life of the sea bass slices, respectively.

4. Conclusion

MEO and/or CuSNP were individually and simultaneously blended with G-CP matrix to prepare multifunctional food wrapping active films. The incorporation of CuSNP and/or MEO could highly improve the antioxidant and antibacterial attributes of G-CP-based films. Thermal analysis revealed that CuSNP had higher melting point then the MEO, Also, by adding CuSNP and MEO to the G-CP films, active films melting point increases. The incorporation of CuSNP and MEO leads to significant changes in the mechanical properties and WVP of G-CP films. The developed active films were characterized utilizing FTIR and XRD. The FTIR and XRD data confirmed that the produced films did not have any side products. Also, besides the single effect of CuSNP and MEO on edible films, their simultaneous use in protein-based films due to the positive synergistic effect between the CuSNP and MEO paves the way for the production of active packaging materials and promises to improve the quality and shelf-life of food products. The results of the physicochemical and microbial analysis of meat samples packed in G-CP films illustrated that the application of G-CP-based films containing CuSNP and MEO could lengthen

561 the shelf-life of the minced meat samples, leading to minimizing the changes in pH, TVN-B,
562 TBA and growing microbial count, thanks to which it could be suggested as a suitable high-
563 performance option in the meat wrapping.

564

565

566

567

568

569

570

571

572

573

574

575

576

577

578

579

Reference

[1] Li, F., Liu, Y., Cao, Y., Zhang, Y., Zhe, T., Guo, Z., ... & Wang, L. (2020). Copper sulfide nanoparticle-carrageenan films for packaging application. *Food Hydrocolloids*, 106094.

[2] Rattaya, S., Benjakul, S., & Prodpran, T. (2009). Properties of fish skin gelatin film incorporated with seaweed extract. *Journal of Food Engineering*, *95*(1), 151-157.

[3] Sani, I. K., Pirsa, S., & Tağı, Ş. (2019). Preparation of chitosan/zinc oxide/Melissa officinalis essential oil nano-composite film and evaluation of physical, mechanical and antimicrobial properties by response surface method. *Polymer Testing*, *79*, 106004.

[4] Tongnuanchan, P., Benjakul, S., Prodpran, T., & Songtipya, P. (2013). Properties and stability of protein-based films from red tilapia (Oreochromis niloticus) protein isolate incorporated with antioxidant during storage. *Food and Bioprocess Technology*, *6*(5), 1113-1126.

[5] Mousazadeh, M., Mousavi, M., Askari, G., Kiani, H., Adt, I., & Gharsallaoui, A. (2018). Thermodynamic and physiochemical insights into chickpea Protein-Persian gum interactions and environmental effects. *International journal of biological macromolecules*, *119*, 1052-1058.

[6] Tongnuanchan, P., Benjakul, S., & Prodpran, T. (2012). Properties and antioxidant activity of fish skin gelatin film incorporated with citrus essential oils. *Food Chemistry*, *134*(3), 1571-1579.

[7] Meshkani, M., Mortazavi, A., & Pourfallah, Z. (2013). Antimicrobial and physical properties of a chickpea protein isolate-based film containing essential oil of thyme using

response surface methodology. *Iranian Journal of Nutrition Sciences & Food Technology*, *8*(1), 93-104.

[8] Zinoviadou, K. G., Gougouli, M., & Biliaderis, C. G. (2016). Innovative biobased materials for packaging sustainability. In *Innovation Strategies in the Food Industry* (pp. 167-189). Academic Press.

[9] Kazemi, M. (2014). Phytochemical composition, antioxidant, anti-inflammatory and antimicrobial activity of Nigella sativa L. essential oil. *Journal of Essential Oil Bearing Plants*, *17*(5), 1002-1011.

[10] Erkan, N., Ayranci, G., & Ayranci, E. (2008). Antioxidant activities of rosemary (Rosmarinus Officinalis L.) extract, blackseed (Nigella sativa L.) essential oil, carnosic acid, rosmarinic acid and sesamol. *Food chemistry*, *110*(1), 76-82.

[11] Dos Santos, C. A., Ingle, A. P., & Rai, M. (2020). The emerging role of metallic nanoparticles in food. *Applied Microbiology and Biotechnology*, *104*(6), 2373-2383.

[12] Sani, I. K., Marand, S. A., Alizadeh, M., Amiri, S., & Asdagh, A. (2020). Thermal, Mechanical, Microstructural and Inhibitory Characteristics of Sodium Caseinate Based Bioactive Films Reinforced by ZnONPs/Encapsulated Melissa officinalis Essential Oil. Journal of Inorganic and Organometallic Polymers and Materials, 1-11.

[13] Roy, S., & Rhim, J. W. (2019). Melanin-mediated synthesis of copper oxide nanoparticles and preparation of functional agar/CuO NP nanocomposite films. *Journal of Nanomaterials*, *2019*.

620 [14] Roy, S., Rhim, J. W., & Jaiswal, L. (2019). Bioactive agar-based functional composite
621 film incorporated with copper sulfide nanoparticles. *Food Hydrocolloids*, *93*, 156-166.

622 [15] Hosseinzadeh, S., Partovi, R., Talebi, F., & Babaei, A. (2020). Chitosan/TiO2
623 nanoparticle/Cymbopogon citratus essential oil film as food packaging material: Physico-
624 mechanical properties and its effects on microbial, chemical, and organoleptic quality of minced
625 meat during refrigeration. *Journal of Food Processing and Preservation*, e14536.

626 [16] Marcous, A., Rasouli, S., & Ardestani, F. (2017). Low-density polyethylene films loaded
627 by titanium dioxide and zinc oxide nanoparticles as a new active packaging system against
628 Escherichia coli O157: H7 in fresh calf minced meat. *Packaging Technology and*
629 *Science*, *30*(11), 693-701.

630 [17] Pirsa, S., Karimi Sani, I., Pirouzifard, M. K., & Erfani, A. (2020). Smart film based on
631 chitosan/Melissa officinalis essences/pomegranate peel extract to detect cream cheeses spoilage.
632 Food Additives & Contaminants: Part A, 37(4), 634-648.

633 [18] Brand-Williams, W., Cuvelier, M. E., & Berset, C. L. W. T. (1995). Use of a free radical
634 method to evaluate antioxidant activity. *LWT-Food science and Technology*, *28*(1), 25-30.

635 [19] Pirsa, S., Karimi Sani, I., & Khodayvandi, S. (2018). Design and fabrication of starch-
636 nano clay composite films loaded with methyl orange and bromocresol green for determination
637 of spoilage in milk package. Polymers for Advanced Technologies, 29(11), 2750-2758.

638 [20] ASTM (1995). Standard test methods for water vapor transmission of material, E 96–95.
639 Annual book of ASTM. Philadelphia, PA: American Society for Testing and Materials.

[21] Chavoshizadeh, S., Pirsa, S., & Mohtarami, F. (2020). Conducting/smart color film based on wheat gluten/chlorophyll/polypyrrole nanocomposite. Food Packaging and Shelf Life, 24, 100501.

[22] Omar-Aziz, M., Khodaiyan, F., Yarmand, M. S., Mousavi, M., Gharaghani, M., Kennedy, J. F., & Hosseini, S. S. (2020a). Combined effects of octenylsuccination and beeswax on pullulan films: Water-resistant and mechanical properties. Carbohydrate Polymers, 255, 117471.

[23] ASTM, Annual Book of ASTM, American Society for Testing and Materials, Philadelphia, 2002, D882-02.

[24] Mehmood, Z., Sadiq, M. B., & Khan, M. R. (2020). Gelatin nanocomposite films incorporated with magnetic iron oxide nanoparticles for shelf life extension of grapes. *Journal of Food Safety*, *40*(4), e12814.

[25] Omar-Aziz, M., Yarmand, M. S., Khodaiyan, F., Mousavi, M., Gharaghani, M., Kennedy, J. F., & Hosseini, S. S. (2020b). Chemical modification of pullulan exopolysaccharide by octenyl succinic anhydride: Optimization, physicochemical, structural and functional properties. *International Journal of Biological Macromolecules*, *164*, 3485-3495.

[26] Gharaghani, M., Mousavi, M., Khodaiyan, F., Yarmand, M. S., Omar-Aziz, M., & Hosseini, S. S. (2020). Octenyl succinylation of kefiran: Preparation, characterization and functional properties. *International Journal of Biological Macromolecules*, *166*, 1197-1209.

[27] Karimi Sani, I., Alizadeh Khaledabad, M., Pirsa, S., & Moghaddas Kia, E. (2020). Physico-chemical, organoleptic, antioxidative and release characteristics of flavoured yoghurt enriched with microencapsulated Melissa officinalis essential oil. International Journal of Dairy Technology, 73(3), 542-551.

662 [28] Vaikousi, H., Biliaderis, C. G., & Koutsoumanis, K. P. (2009). Applicability of a
663 microbial Time Temperature Indicator (TTI) for monitoring spoilage of modified atmosphere
664 packed minced meat. *International Journal of Food Microbiology*, *133*(3), 272-278.

665 [29] Kirk, S., & Sawyer, R. (1991). *Pearson's composition and analysis of foods* (No. Ed. 9).
666 Longman Group Ltd.

667 [30] AOAC. (1995). Official methods of analysis of the AOAC international (16th ed.).
668 Rockville, MD: AOAC International.

669 [31] Asdagh, A., & Pirsa, S. (2020a). Bacterial and oxidative control of local butter with
670 smart/active film based on pectin/nanoclay/Carum copticum essential oils/β-
671 carotene. *International Journal of Biological Macromolecules*, *165*, 156-168.

672 [32] Kadam, D., Shah, N., Palamthodi, S., & Lele, S. S. (2018). An investigation on the effect
673 of polyphenolic extracts of Nigella sativa seedcake on physicochemical properties of chitosan-
674 based films. *Carbohydrate polymers*, *192*, 347-355.

675 [33] Akloul, R., Benkaci-Ali, F., Zerrouki, M., & Eppe, G. (2014). Composition and biological
676 activities of the essential oil of Nigella sativa seeds isolated by accelerated microwave steam
677 distillation with cryogenic grinding. American Journal of Essential Oils and Natural
678 Products, 1(3), 23-33.

679 [34] Hosseini, S. F., Rezaei, M., Zandi, M., & Farahmandghavi, F. (2016). Development of
680 bioactive fish gelatin/chitosan nanoparticles composite films with antimicrobial properties. *Food*
681 *Chemistry*, *194*, 1266-1274.

[35] Asdagh, A., Sani, I. K., Pirsa, S., Amiri, S., Shariatifar, N., Eghbaljoo–Gharehgheshlaghi, H., ... & Taniyan, A. (2020b). Production and characterization of nanocomposite film based on whey protein isolated/copper oxide nanoparticles containing coconut essential oil and paprika extract. *Journal of Polymers and the Environment*, 1-15.

[36] Zhang, W., & Jiang, W. (2020). Antioxidant and antibacterial chitosan film with tea polyphenols-mediated green synthesis silver nanoparticle via a novel one-pot method. *International journal of biological macromolecules*, *155*, 1252-1261.

[37] Qin, Y., Liu, Y., Yuan, L., Yong, H., & Liu, J. (2019). Preparation and characterization of antioxidant, antimicrobial and pH-sensitive films based on chitosan, silver nanoparticles and purple corn extract. *Food Hydrocolloids*, *96*, 102-111.

[38] Roy, S., & Rhim, J. W. (2020). Effect of CuS reinforcement on the mechanical, water vapor barrier, UV-light barrier, and antibacterial properties of alginate-based composite films. *International Journal of Biological Macromolecules*, *164*, 37-44.

[39] Ekramian, S., Abbaspour, H., Roudi, B., Amjad, L., & Nafchi, A. M. (2020). Influence of Nigella sativa L. Extract on Physico−Mechanical and Antimicrobial Properties of Sago Starch Film. *Journal of Polymers and the Environment*, 1-8.

[40] Taqi, A., Askar, K. A., Mutihac, L., & Stamatin, I. (2013). Effect of Laurus nobilis L. oil, Nigella sativa L. oil and oleic acid on the antimicrobial and physical properties of subsistence agriculture: the case of cassava/pectin based edible films. *Food and agricultural immunology*, *24*(2), 241-254.

[41] Rohman, A., Wibowo, D., Sudjadi, Lukitaningsih, E., & Rosman, A. S. (2015). Use of fourier transform infrared spectroscopy in combination with partial least square for authentication of black seed oil. *International Journal of Food Properties*, *18*(4), 775-784.

[42] Huntrakul, K., Yoksan, R., Sane, A., & Harnkarnsujarit, N. (2020). Effects of pea protein on properties of cassava starch edible films produced by blown-film extrusion for oil packaging. *Food Packaging and Shelf Life*, *24*, 100480.

[43] Kaewprachu, P., Osako, K., Benjakul, S., & Rawdkuen, S. (2015). Quality attributes of minced pork wrapped with catechin–lysozyme incorporated gelatin film. *Food Packaging and Shelf Life*, *3*, 88-96.

[44] Rezaei, F., & Shahbazi, Y. (2018). Shelf-life extension and quality attributes of sauced silver carp fillet: A comparison among direct addition, edible coating and biodegradable film. *LWT*, *87*, 122-133.

[45] Tabatabaee Bafroee, A. S., Khanjari, A., Teimourifard, R., & Yarmahmoudi, F. (2020). Development of a novel active packaging film to retain quality and prolong the shelf life of fresh minced lamb meat. *Journal of Food Processing and Preservation*, *44*(11), e14880.

[46] Arfat, Y. A., Benjakul, S., Vongkamjan, K., Sumpavapol, P., & Yarnpakdee, S. (2015). Shelf-life extension of refrigerated sea bass slices wrapped with fish protein isolate/fish skin gelatin-ZnO nanocomposite film incorporated with basil leaf essential oil. *Journal of food science and technology*, *52*(10), 6182-6193.

[47] Artharn, A., Prodpran, T., & Benjakul, S. (2009). Round scad protein-based film: Storage stability and its effectiveness for shelf-life extension of dried fish powder. *LWT-Food Science and Technology*, *42*(7), 1238-1244.

[48] Gómez-Estaca, J., De Lacey, A. L., López-Caballero, M. E., Gómez-Guillén, M. C., & Montero, P. (2010). Biodegradable gelatin–chitosan films incorporated with essential oils as antimicrobial agents for fish preservation. *Food microbiology*, *27*(7), 889-896.

[49] Ahmad, M., Benjakul, S., Sumpavapol, P., & Nirmal, N. P. (2012). Quality changes of sea bass slices wrapped with gelatin film incorporated with lemongrass essential oil. *International Journal of Food Microbiology*, *155*(3), 171-178.

743 **Figures captions**

744 Fig. 1. 3-Dimensional plots of the effect of MEO and CuSNP on the thickness, antioxidant,
745 WVP and moisture content of G-CP/MEO/CuSNP film.

746 Fig. 2. 3-Dimensional plots of the effect of MEO and CuSNP on the color properties of G-
747 CP/MEO/CuSNP film.

748 Fig. 3. FTIR (A) CP(a)-G(b)- MEO(c)- CuSNP(d)- G-CP(e) - G-CP-MEO 0.5(f)- G-CP-CuSNP
749 0.03(g)- G-CP-MEO 0.5-CuSNP 0.03(h), X-ray(B) G-CP(a) - G-CP-MEO 0.5(b)- G-CP-CuSNP
750 0.03(c)- G-CP-MEO 0.5-CuSNP 0.03(d) and scanning electron micrograph(C) G-CP(a) - G-CP-
751 MEO 0.5(b)- G-CP-CuSNP 0.03(c)- G-CP-MEO 0.5-CuSNP 0.03(d) of surface of the film
752 samples.

753

754

755

756

757

758

759

760

761

762

Table 1

List of Experiments in the CCD

Run	MEO (W/V)	CuSNP (W/V)
1*	0	0
2	0.25	0
3*	0.5	0
4	0	0.015
5*	0	0.03
6	0.25	0.015
7	0.25	0.03
8	0.5	0.015
9*	0.5	0.03
10	0.25	0.015
11	0.25	0.015
12	0.25	0.015
13	0.25	0.015

* Treatments that were used in a factorial design (These treatments were performed in three replications)

Table 2

Some characteristics of the constructed models for responses

Response	Regression equation	Model summary
Thickness	Thickness= 0.13 + 0.023 MEO - 0.43 CuSNP	R-sq = 0.76
RSA	RSA= 13.63 - 69.53 MEO + 2610.16 CuSNP - 2722.67 MEO * CuSNP + 244.68 MEO^2 - 28075.9 $CuSNP^2$	R-sq = 0.91
WVP	WVP= 13.99 - 2.83 MEO - 264.82 CuSNP – 8 MEO * CuSNP + 12.085 MEO^2 + 6557.08 $CuSNP^2$	R-sq = 0.76
Moisture	Moisture Content= 22.14 - 9.42 MEO - 112.55 CuSNP + 345.33 MEO * CuSNP	R-sq = 0.71
L*	L*= L* =89.72+0.62MEO -1838.02 CuSNP +256.66 MEO * ZrO2 -8.35 MEO^2 +35058.23 CuSNP	R-sq = 0.99
a*	a*= -3.69 - 19.04 MEO + 3178.85 CuSNP - 83.33 MEO * CuSNP + 32.97 MEO^2 - 59130.3 $CuSNP^2$	R-sq = 0.99
b*	b*= 2.80 + 44.85 MEO + 8458.41 CuSNP - 737.3 MEO * CuSNP - 64.46 MEO^2 - $CuSNP^2$	R-sq = 0.99
ΔE	ΔE= 22.08 + 255.63 MEO + 6778.64 CuSNP - 5706.67 MEO * CuSNP - 233.77 MEO^2 - $CuSNP^2$	R-sq = 0.88

Table 3

Tensile strength (TS), Elongation at break (EAB) and antibacterial activity of G-CP films containing MEO and CuSNP

Films	TS (MPa)	EAB (%)	Diameter of inhibition zone (mm)	
			S. aureus	*E. coli*
G-CP	10.42 ± 0.11^{a}	7.68 ± 0.12^{c}	7.06 ± 0.08^{d}	7.16 ± 0.17^{c}
G-CP-MEO 0.5	6.38 ± 0.21^{d}	12.96 ± 0.08^{a}	24.45 ± 0.12^{b}	18.30 ± 0.13^{b}
G-CP-CuSNP 0.03	7.02 ± 0.08^{c}	3.44 ± 0.03^{d}	15 ± 0.19^{c}	20.00 ± 0.14^{b}
G-CP-MEO 0.5-CuSNP 0.03	8.56 ± 0.18^{b}	9.33 ± 0.31^{b}	27.11 ± 0.35^{a}	33.40 ± 0.28^{a}

Different letters in the same column indicate significant differences ($P < 0.05$)

Table 4

Effect of MEO and CuSNP on melting temperature (Tm) and glass transition temperature (Tg) of G-CP based film.

Samples	Tm (ºC)	Tg
G-CP	88.07	3.2
G-CP-MEO 0.5	133.38	35.4
G-CP-CuSNP 0.03	188.15	41.67
G-CP-MEO 0.5-CuSNP 0.03	194.5	48.17

Table 5

Physicochemical and bacteriological analysis of minced meat samples wrapped with G-CP films incorporated with MEO and CuSNP during storage at 4 °C for 14 days.

Test	Samples	Days of storage (days)			
		1	4	8	14
pH	G-CP	5.85 ± 0.65^{a}	6.1 ± 0.89^{a}	6.20 ± 0.87^{a}	6.35 ± 0.76^{a}
	G-CP-MEO 0.5	5.85 ± 0.87^{a}	5.9 ± 0.65^{b}	5.97 ± 0.98^{b}	6.1 ± 0.56^{b}
	G-CP-CuSNP 0.03	5.85 ± 0.23^{a}	5.9 ± 0.78^{b}	5.95 ± 0.76^{b}	5.99 ± 0.13^{c}
	G-CP-MEO 0.5-CuSNP 0.03	5.85 ± 0.41^{a}	5.8 ± 0.58^{c}	5.9 ± 0.89^{c}	5.93 ± 0.16^{d}
TBA mg (MDA/kg)	G-CP	0.4 ± 0.00^{a}	1.8 ± 0.01^{a}	2.2 ± 0.02^{a}	2.6 ± 0.04^{a}
	G-CP-MEO 0.5	0.4 ± 0.00^{a}	0.9 ± 0.01^{c}	1.1 ± 0.01^{b}	1.3 ± 0.01^{c}
	G-CP-CuSNP 0.03	0.4 ± 0.00^{a}	1.1 ± 0.00^{b}	1.3 ± 0.01^{b}	1.6 ± 0.02^{b}
	G-CP-MEO 0.5-CuSNP 0.03	0.4 ± 0.00^{a}	0.8 ± 0.00^{c}	1 ± 0.00^{c}	1.1 ± 0.01^{c}
TVB-N mg (N/100 g)	G-CP	7 ± 0.85^{a}	19 ± 0.76^{a}	26 ± 0.54^{a}	37 ± 0.89^{a}
	G-CP-MEO 0.5	7 ± 0.23^{a}	12 ± 0.98^{b}	15 ± 0.64^{b}	19 ± 0.63^{c}
	G-CP-CuSNP 0.03	7 ± 0.34^{a}	14 ± 0.38^{b}	17 ± 0.58^{b}	25 ± 0.45^{b}
	G-CP-MEO 0.5-CuSNP 0.03	7 ± 0.56^{a}	9 ± 0.74^{c}	12 ± 0.76^{c}	18 ± 0.33^{c}
L. monocytogenes log(cfu/g)	G-CP	5 ± 0.01^{a}	5.5 ± 0.02^{a}	5.9 ± 0.06^{a}	6.7 ± 0.07^{a}
	G-CP-MEO 0.5	5 ± 0.02^{a}	3.4 ± 0.03^{c}	3.1 ± 0.01^{c}	2.7 ± 0.01^{c}
	G-CP-CuSNP 0.03	5 ± 0.07^{a}	4.1 ± 0.05^{b}	3.8 ± 0.03^{b}	3.4 ± 0.02^{b}
	G-CP-MEO 0.5-CuSNP 0.03	5 ± 0.03^{a}	3.1 ± 0.01^{d}	3.0 ± 0.04^{c}	2.2 ± 0.01^{d}
***S. aureus* log(cfu/g)**	G-CP	1.56 ± 0.01^{a}	3.2 ± 0.06^{a}	3.47 ± 0.07^{a}	5.15 ± 0.03^{a}
	G-CP-MEO 0.5	1.5 ± 0.02^{b}	2.11 ± 0.03^{b}	2.27 ± 0.03^{b}	2.4 ± 0.03^{b}
	G-CP-CuSNP 0.03	1.47 ± 0.03^{c}	2.3 ± 0.02^{c}	2.39 ± 0.02^{b}	2.59 ± 0.02^{b}
	G-CP-MEO 0.5-CuSNP 0.03	1.55 ± 0.04^{a}	2 ± 0.01^{d}	2.14 ± 0.02^{c}	2.16 ± 0.03^{d}
Enterobacteriaceae log(cfu/g)	G-CP	2.6 ± 0.01^{a}	4.1 ± 0.06^{a}	4.8 ± 0.02^{a}	5.9 ± 0.05^{a}
	G-CP-MEO 0.5	2.6 ± 0.02^{a}	3.4 ± 0.03^{b}	3.7 ± 0.01^{b}	4.8 ± 0.03^{b}
	G-CP-CuSNP 0.03	2.6 ± 0.03^{a}	3 ± 0.04^{c}	3.3 ± 0.07^{b}	4.4 ± 0.01^{b}
	G-CP-MEO 0.5-CuSNP 0.03	2.6 ± 0.01^{a}	2.8 ± 0.01^{d}	3 ± 0.04^{c}	3.8 ± 0.03^{c}
***Pseudomonas spp.* log(cfu/g)**	G-CP	2.9 ± 0.02^{a}	5.4 ± 0.03^{a}	6 ± 0.08^{a}	7.8 ± 0.04^{a}
	G-CP-MEO 0.5	2.9 ± 0.01^{a}	3.5 ± 0.02^{b}	4 ± 0.03^{b}	4.8 ± 0.09^{b}
	G-CP-CuSNP 0.03	2.9 ± 0.04^{a}	3.3 ± 0.01^{b}	3.8 ± 0.01^{b}	4.7 ± 0.01^{b}
	G-CP-MEO 0.5-CuSNP 0.03	2.9 ± 0.01^{a}	3 ± 0.04^{c}	3.4 ± 0.04^{c}	4.4 ± 0.03^{b}

Different letters in the same column indicate significant differences ($P < 0.05$)

Figures

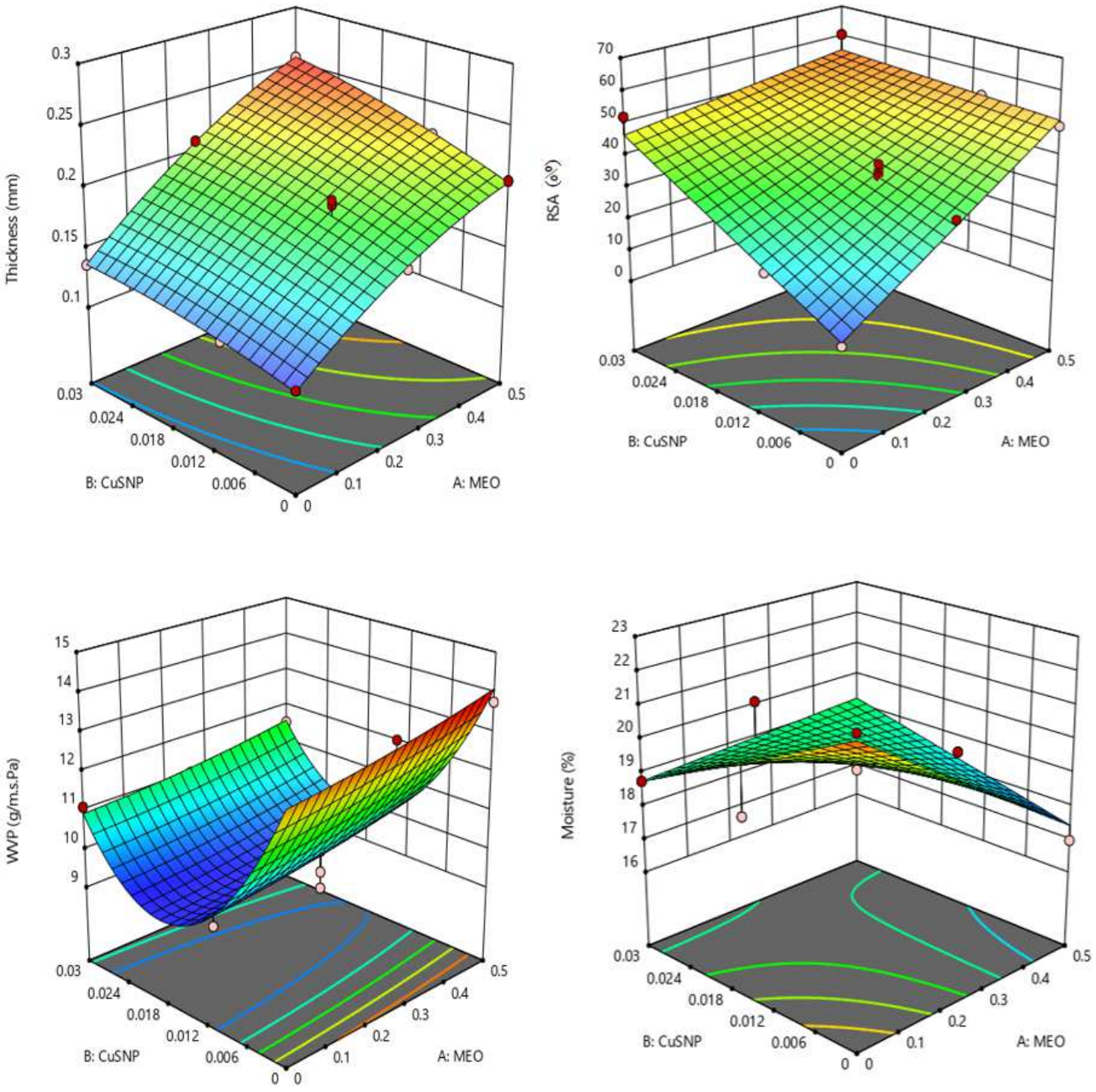

Figure 1

3-Dimensional plots of the effect of MEO and CuSNP on the thickness, antioxidant, WVP and moisture content of G-CP/MEO/CuSNP film.

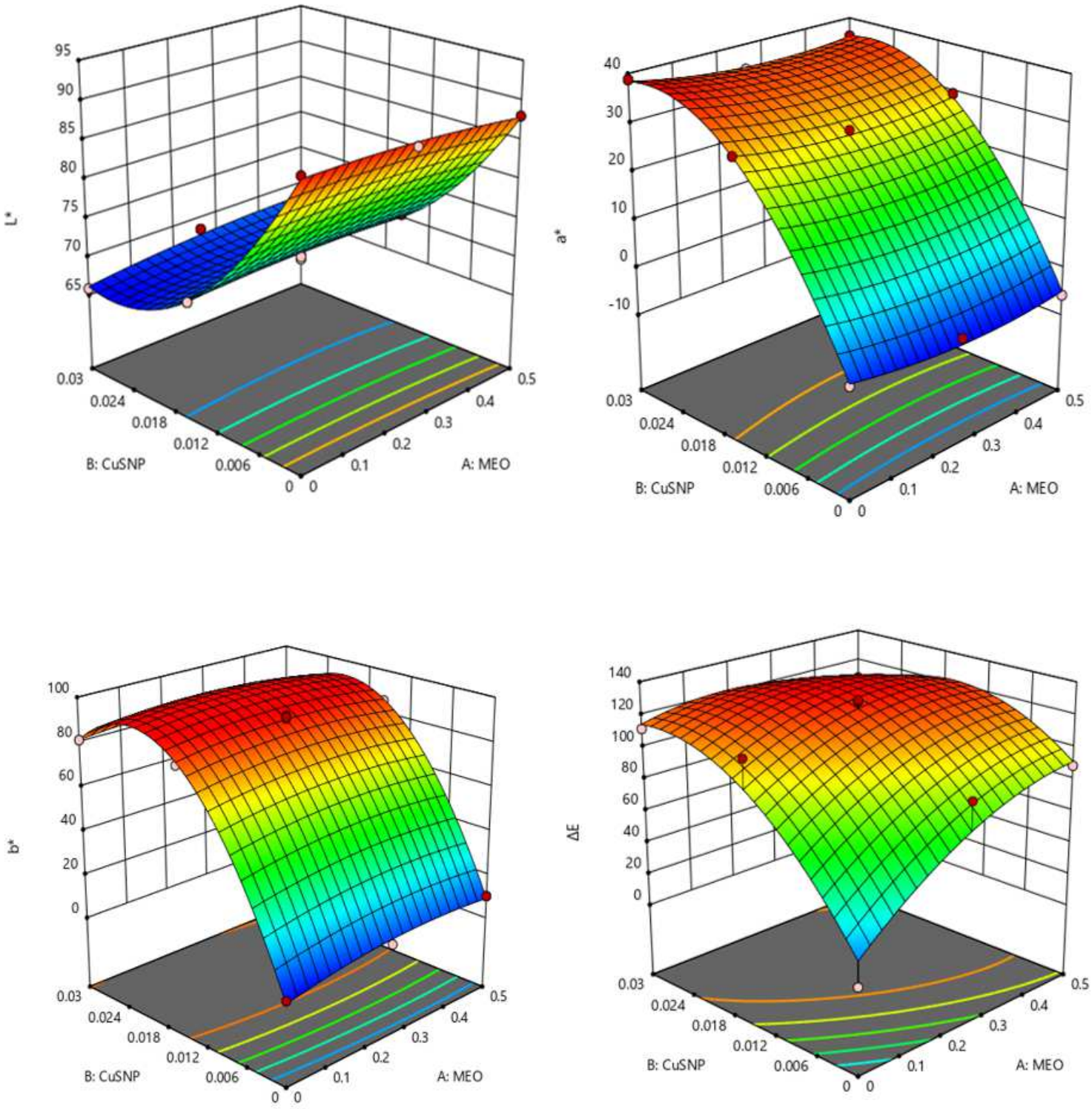

Figure 2

3-Dimensional plots of the effect of MEO and CuSNP on the color properties of G-CP/MEO/CuSNP film.

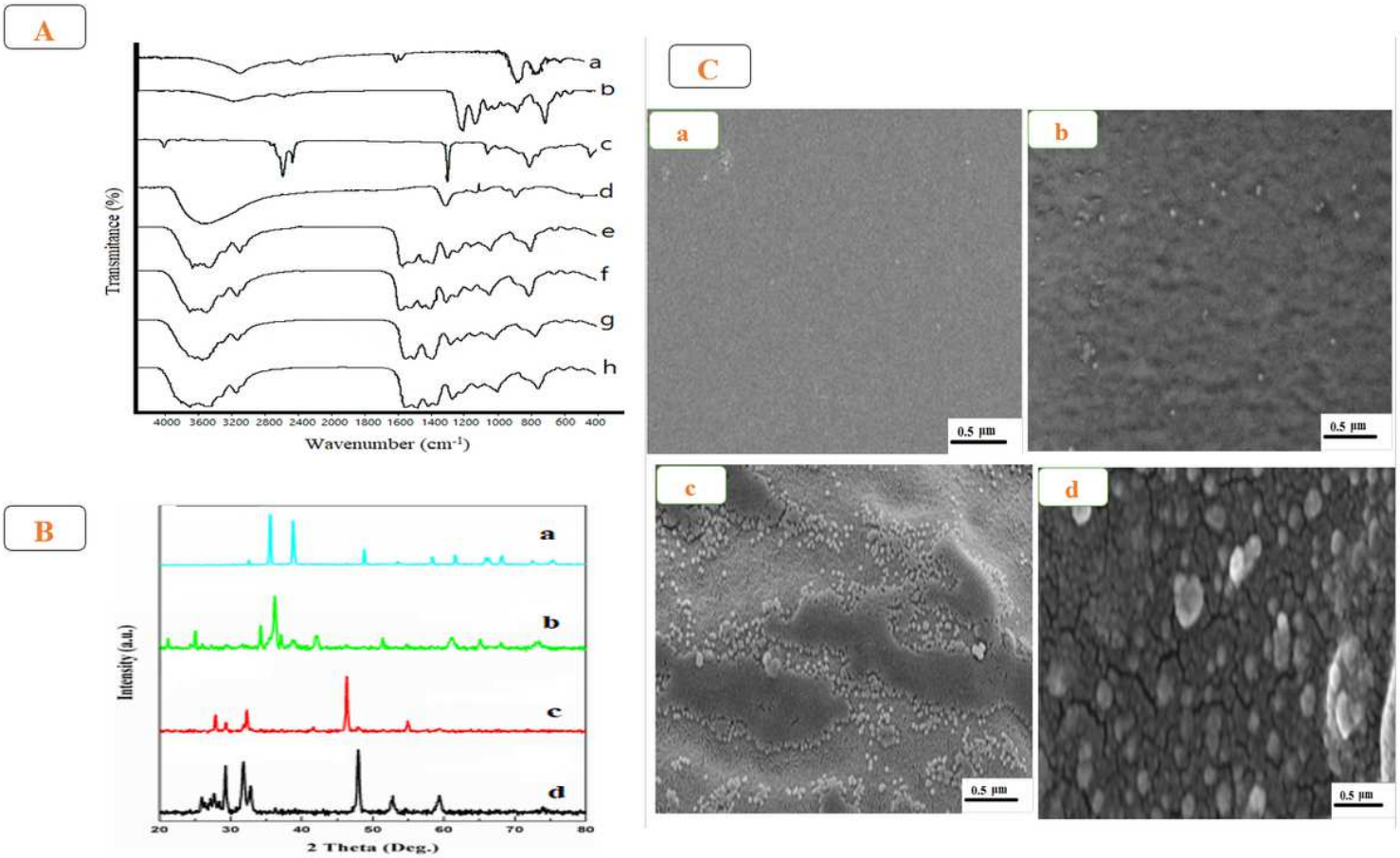

Figure 3

FTIR (A) CP(a)-G(b)- MEO(c)- CuSNP(d)- G-CP(e) - G-CP-MEO 0.5(f)- G-CP-CuSNP 0.03(g)- G-CP-MEO 0.5-CuSNP 0.03(h), X-ray(B) G-CP(a) - G-CP-MEO 0.5(b)- G-CP-CuSNP 0.03(c)- G-CP-MEO 0.5-CuSNP 0.03(d) and scanning electron micrograph(C) G-CP(a) - G-CP-MEO 0.5(b)- G-CP-CuSNP 0.03(c)- G-CP-MEO 0.5-CuSNP 0.03(d) of surface of the film samples.